Fast prompt-gamma imaging for the online monitoring of the ion range in hadron therapy

Jayde Livingstone[1,2], Ane Extebeste[3], Sidiki Malick Cissé[1], Denis Dauvergne[1], Mattia Fontana[2], Marie-Laure Gallin-Martel[1], Jean-Michel Létang[3], Sara Marcatili[1], Christian Morel[4], David Sarrut[3] & Etienne Testa[2]

1. Université Grenoble Alpes, Laboratoire de Physique Subatomique et de Cosmologie, CNRS/IN2P3, Grenoble, France
2. Université de Lyon, Institut de Physique Nucléaire de Lyon, CNRS/IN2P3, Lyon, France
3. INSA CREATIS, CNRS/INSERM, Lyon France
4. Aix-Marseille Univ, CNRS/IN2P3, CPPM, Marseille, France

e-mail: jayde.livingstone@lpsc.in2p3.fr

Range uncertainties in hadron therapy

Ion range uncertainties in hadron therapy may arise from [1, 2]:

- patient mispositioning
- changes in patient anatomy or tumour morphology
- the conversion of Hounsfield units to ion stopping power

For proton therapy conservative margins are often placed on the Planning Treatment Volume (PTV), which may be as large as a centimeter for deep seated tumours [3]. Since the distal edge of the Bragg peak is not used to define the field, treatments are often performed using several fields where one could be sufficient.

The ballistic properties of protons are thus not fully exploited!

Online monitoring via prompt γ imaging

Secondary particles, including prompt γ-rays, are emitted as a result of interactions between primary protons and target nuclei.

- The spatial distribution of γ emission is closely correlated with the proton range [1], Fig. 1
- γ-rays can be discriminated from neutrons and other particles using time of flight (TOF)
- A method of measuring the γ emission vertex distribution is by using a Compton camera

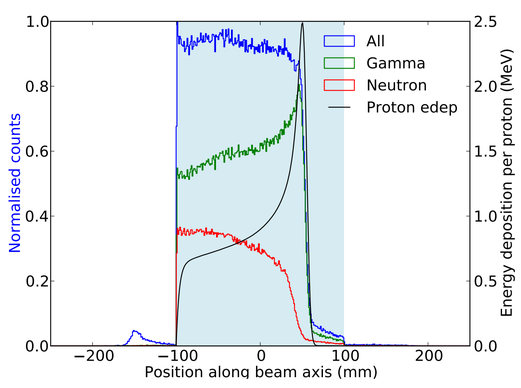

Fig. 1: Energy deposition of 160 MeV protons in a PMMA phantom (shaded area) and distributions of secondary particles along proton beam axis.

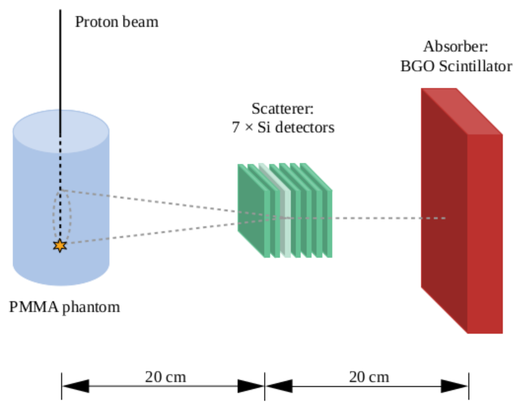

Fig. 2: Geometry of the CLaRyS Compton camera. The star represents a γ emission vertex.

The CLaRyS Compton camera:

scatterer 7 parallel plane silicon detectors; $9 \times 9 \times 0.2$ cm^3

absorber BGO scintillating detector; $35 \times 35 \times 3$ cm^3

Using the Compton equation, a conical surface (with opening angle 2θ) on which the emission vertex lies is constructed.

$$\cos\theta = 1 - m_e c^2 \left(\frac{1}{E_{abs}} - \frac{1}{(E_{scat}+E_{abs})}\right)$$

E_{scat} and E_{abs} are the energies deposited in the scatterer and absorber respectively by a secondary photon.

Methods of reconstructing the γ emission vertex:

Method	Description	Advantage	Disadvantage
Iterative	Most likely emission vertex based on intersection of many cones	2 mm precision for 10^7 primary particles [4]	Slow, requires a lot of computing resources
Line-cone intersection	Two solutions resulting from intersection of line (proton trajectory) and Compton cone	Much faster due to simplified algorithm	$\sim$3$\times$ worse precision [4] due to inability to distinguish between two solutions

Hypothesis: With an ultra-fast time resolution ($\sim$100 ps), one of the line-cone solutions can be rejected, thus improving the precision of the range measurement.

Damavan Temporal $CeBr_3$ Compton camera

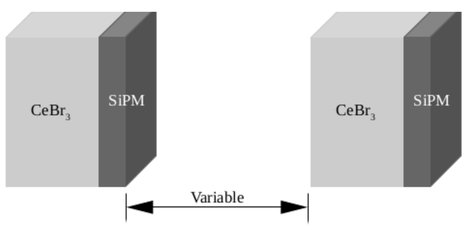

Fig. 3: Geometry of the Temporal camera.

- Two $CeBr_3$ scintillators, each coupled to an SiPM matrix
- The sampling of the scintillation light collection in the crystal is used to calculate location of every γ ray interaction in 3D with high spatial resolution (2 mm)
- The quoted temporal resolution is $\sim$100 ps RMS
- http://damavan-imaging.com/cebr3-detector-fluoral-technology/

The Temporal detector has been calibrated and characterised for its energy resolution and angular dependence of the energy resolution using sealed sources of ^{22}Na, ^{60}Co and ^{152}Eu.

GATE simulations of CLaRyS Compton camera

Simulations have been performed using GATE version 7 (Geant4 10.03.p03).

Physics list QGSP_BIC_HP hadronic physics, Livermore electromagnetic physics

Source 5 mm diameter proton beam of 160 MeV, 10^9 particles

Actor GateComptonCameraActor, 40 ns coincidence window

Proposed method of solution discrimination based on time of flight (TOF):
For each solution a TOF is estimated ($TOF_{est} = TOF_{proton} + TOF_{\gamma}$) and compared to the real TOF (TOF_{CC}). The solution for which ΔTOF (TOF_{CC} - TOF_{est}) is smallest is selected. Additional criteria are used to simulate the temporal resolution.

Effect of temporal resolution on line-cone reconstruction

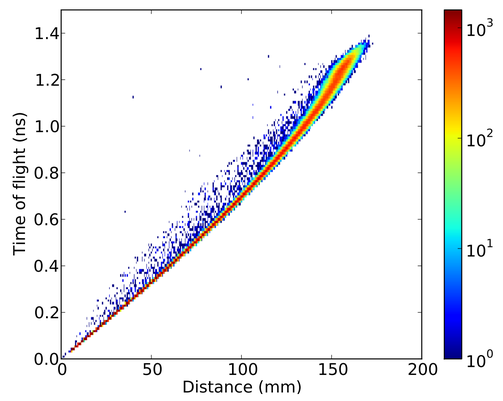

Fig. 4: Time of γ creation as a function of distance from hodoscope.

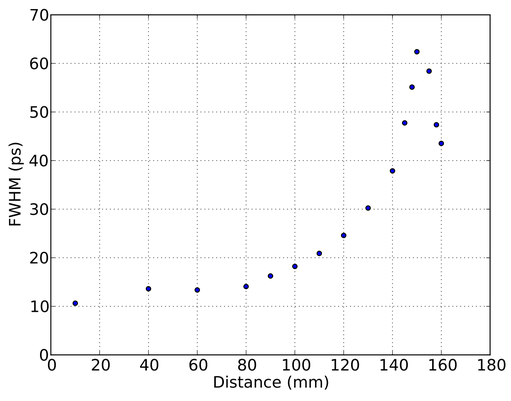

Fig. 5: Spread in the time of γ creation as a function of distance from the hodoscope.

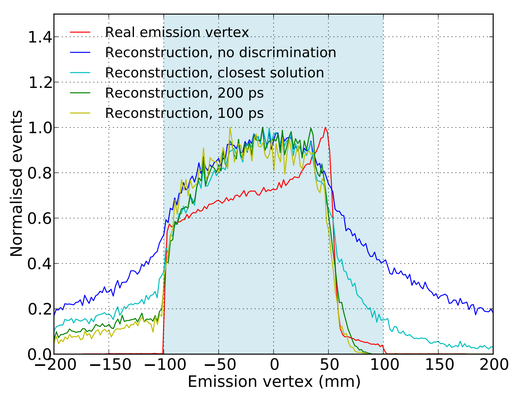

Fig. 6: The real γ emission vertex along the beam axis compared to reconstructions with different criteria.

- The maximum spread in time of γ creation is 62 ps at a distance of 150 mm from the hodoscope
- Method is efficient at removing noise beyond distal fall-off of real emission vertex peak
- Solution discrimination results in a reduction of statistics ($\sim$2 for $\Delta TOF \leq$ 100 ps compared to ΔTOF_{min}
- The precision of the ion range measured will be quantitatively assessed
- The origin of reconstructed events upstream of the phantom is also being investigated

Characterisation of Temporal camera

- The detector exhibits a linear response with energy (0.25–1.4 MeV)
- The energy resolution is constant as a function of angle of source from camera
- The temporal resolution will be studied

Energy (MeV)	Resolution FWHM (%)
0.25	28
0.53	10.8
0.97	11.1
1.17	7.6
1.33	6.5

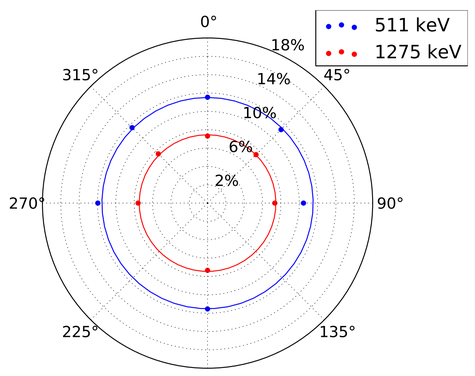

Fig. 7: Energy resolution as a function of angle.

Conclusion

High temporal resolution, of the order of 100 ps, improves the precision of ion range determination using a Compton camera and it is envisaged that the CLaRyS Compton camera will be upgraded with an ultra-fast scintillator such as $CeBr_3$. The authors aknowledge ITMO-Cancer (CLaRyS-UFT project) and LabEx PRIMES (ANR-11-LABX-0063).

References

[1] J. Krimmer, *et al.*, *Nucl. Instrum. Methods Phys. Res. A*, vol. 878, pp. 58–73, 2017.

[2] A. C. Knopf and A. Lomax, *Phys. Med. Biol*, vol. 58, R131, 2013.

[3] H. Paganetti, *Phys. Med. Biol.*, vol. 57, pp. R99–R117, 2012.

[4] M. Fontana, *et al.*, submitted to *IEEE Trans. Radiat. Plasma Med. Sci.*, 2019.